20th International Conference on Structural Mechanics in Reactor Technology (SMiRT 20)
Espoo, Finland, August 9-14, 2009
SMiRT 20-Division II, Paper 1899

Evaluation of J-Integral for Surface Cracked Plates Under Biaxial Tensile/Bending Loading Using Extended Reference Stress Method

Naoki Miua [a], Yukio Takahashi [a]

[a] *Central Research Institute of Electric Power Industry, Yokosuka, Japan, e-mail: miura@criepi.denken.or.jp*

Keywords: J-Integral, Limit Moment, Reference Stress Method, Biaxial Loading, Surface Cracks.

1 ABSTRACT

In this paper, reference stress solutions for plates with semi-elliptical surface cracks were reviewed, and the applicability of the solutions was examined through the comparison with finite element analysis results under uniaxial loading. Next, an extended reference stress method was newly developed to evaluate J-integral for cracked plates under biaxial tensile and/or bending loading. The accuracy of the method was validated through the comparison with finite element analysis results under biaxial loading.

2 INTRODUCTION

Conventional creep-fatigue crack growth analysis or unstable fracture analysis has been conducted under uniaxial stress condition. However, actual plant components come into various multiaxial stress conditions. Therefore, the evaluation of fracture mechanics parameter of cracked bodies under multiaxial stress conditions is essentially needed for the accurate estimation of crack growth behavior and fracture behavior. The authors proposed the extended reference stress method to evaluate J-integral for surface cracked plates subjected to remote tensile load perpendicular to the crack and remote tensile/compressive load parallel to the crack at the same time (Miura and Takahashi, 2007).

In this paper, an extend reference stress method applicable to general biaxial loading was investigated. Three-dimensional finite element analysis for surface cracked plates subjected to biaxial loading was conducted to see the effect of biaxial loading on J-integral. An extended reference stress method was then proposed to evaluate J-integral for surface cracked plates subjected to remote bending and tensile load perpendicular to the crack and remote tensile/compressive load parallel to the crack at the same time, and the applicability of the proposed method was validated through the comparison with the results of the finite element analysis.

3 REFERENCE STRESS SOLUTIONS FOR SURFACE CRACKED PLATES

3.1 Review of reference stress solutions and derivation of limit load solutions

Several reference stress solutions have been proposed for plates with a semi-elliptical surface crack subjected to "uniaxial" tension and bending, based on individual theoretical model, yield condition, and numerical analysis (Willoughby and Davey, 1989, Sattari-Far, 1994, Sattari-Far and Dillström, 2004, Goodall and Webster, 2001, and Lei, 2004). The reference stress, σ_{ref}, can be generally expressed as

$$\sigma_{ref} = f\left(\sigma_m, \sigma_b, \frac{a}{t}, \frac{a}{c}, \frac{c}{b}\right) \tag{1}$$

where σ_m and σ_b are the membrane stress and the bending stress applied to the plate, a and c are the crack depth and the half crack length, and t and b are the plate thickness and the half plate width, respectively.

Considering that surface cracked plates are subjected to bending moment, M, and tensile load, P, the limit moment, M_L, can be estimated by the following equation using σ_{ref} and the yield stress, σ_Y.

$$M_L = \frac{\sigma_Y}{\sigma_{ref}} M \qquad (2)$$

The bending moment, M, and the limit moment for uncracked plate, M_{L0}, is given by

$$M = \frac{1}{3} b t^2 \sigma_b \qquad (3)$$

$$M_{L0} = \frac{1}{2}\frac{1}{k} b t^2 \sigma_Y, \quad k = \frac{1}{4}\left(\sqrt{4+\Lambda^2}+2\right) \qquad (4)$$

where Λ (= $6\sigma_m/\sigma_b = Pt/M$) is the tension-bending ratio. Thus the normalized limit moment, M_L/M_{L0}, can be calculated by

$$\frac{M_L}{M_{L0}} = \frac{2}{3} k \frac{\sigma_b}{\sigma_{ref}} \qquad (5)$$

Following the above procedure, the existing reference stress solutions can be replaced with the limit moment solutions for surface cracked plates subjected to combined tension and bending.

3.2 Availability of limit moment solutions

Figs. 1(a) to (d) show the comparison of the normalized limit moments under pure bending and combined bending and tension based on the existing reference stress solutions and obtained from the elastic-perfectly plastic finite element analysis (see the later section for detailed analysis condition). The solutions by Willoughby (1989) and Sattari-Far (1994) give excessively small limit moments. In contrast, the solutions by Sattari-Far and Dillström (2004), and Lei (2004) (which is identical with Goodall and Webster (2001)) seem to provide reasonable relations between M_L/M_{L0} and a/t. Assuming that the finite element results are

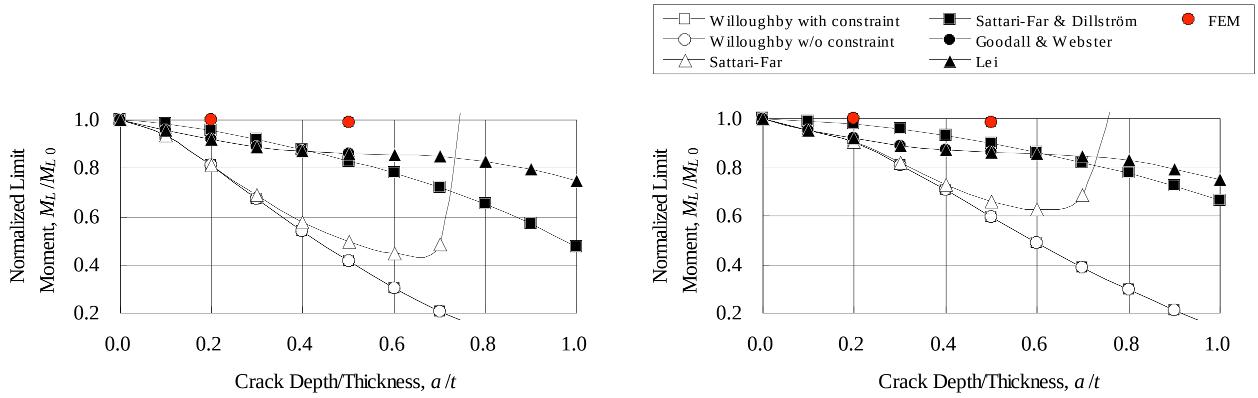

(a) Pure bending, a/c = 0.2, c/b = 0.25

(b) Pure bending, a/c = 0.6, c/b = 0.25

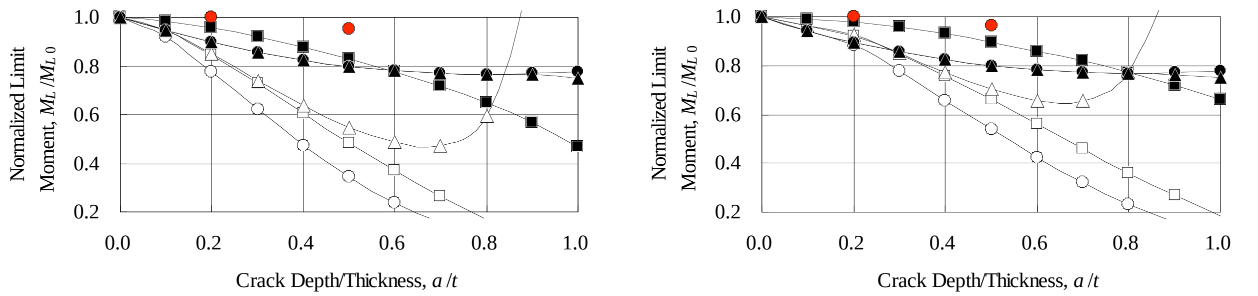

(c) Combined loading (Λ = 3), a/c = 0.2, c/b = 0.25

(d) Combined loading (Λ = 3) a/c = 0.6, c/b = 0.25

Figure 1. Comparison of normalized limit moments

exact, the average error of the predicted M_L/M_{L0} was 7% for the Sattari-Far and Dillström solution and 12% for the Lei solution.

4 FINITE ELEMENT ANALYSIS UNDER BIAXIAL LOADING

4.1 Analysis condition

Three-dimensional finite element analyses of surface cracked plates were conducted. Fig. 2 shows the analysis model. The half plate width, b, the half plate length, L, and the half crack length, c, were fixed to 100 mm, 400 mm, and 25 mm, respectively. The aspect ratio, a/c, was set to 0.2 and 0.6, and the normalized crack depth, a/t, was set to 0.2 and 0.5. Table 1 (a) shows the list of crack sizes.

The analysis was conducted using "MARC" with twenty-noded solid elements. The remote bending stress, S_{yb}, and the remote membrane stress, S_{ym}, perpendicular to the crack, and the remote membrane stress parallel to the crack, S_x, were applied. The final S_{yb} was fixed to 200 MPa, the final Sym was set to 0 and 100 MPa, and the final S_x was varied from -100 to 100 MPa. The stresses were loaded proportionally. Table 1 (b) shows the list of loading conditions. The results on Cases A and D in the table were used in the preceding section to see the availability of the limit moment solutions under uniaxial loading.

Two types of stress-strain relations were prepared. One was the elastic-perfectly plastic stress-strain relation, whose results were used to validate the proposed limit moment solution under biaxial loading, and the other was elastic-plastic stress-strain relation, whose results were applied to validate the proposed J-evaluation method under biaxial loading. Table 2 shows the material properties used in the analyses. For the elastic-plastic analysis, J-integrals both at the deepest points and at the surface points were evaluated by path-integrals. Fig. 3 shows an example of finite element mesh.

4.2 Results of elastic-perfectly plastic analysis

An example relation between S_{yb} and crack-opening displacement (COD) for Case 1 (a/c = 0.2, a/t = 0.5) is shown in Fig. 4. The relations in smaller COD ranges show almost identical curves in spite of the different S_x/S_{yb} or S_{ym}/S_{yb}. The values of S_{yb} converge to a constant level at larger COD, which are corresponding to the limit moment on the global yielding.

Fig. 5 shows the relation between the normalized limit moment, $M_{L,biaxial}/M_{L,uniaxial}$, and S_x/S_{yb}, where $M_{L,biaxial}$ is the limit moment obtained from the analysis for a specific S_x/S_{yb}, and $M_{L,biaxial}$ is the limit moment at S_x = 0. The normalized limit moment is not significantly affected by a/t or a/c. It takes the maximum values at S_x/S_{yb} = 0 for pure bending perpendicular to the crack, and at S_x/S_{yb} = 0.5 for combined loading perpendicular to the crack. This suggests that the limit moment under biaxial loading is affected by S_x/S_{yb} as well as the combination of S_{ym} and S_{yb}.

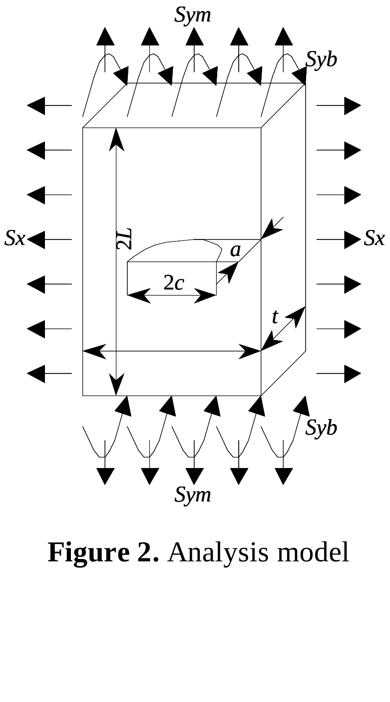

Figure 2. Analysis model

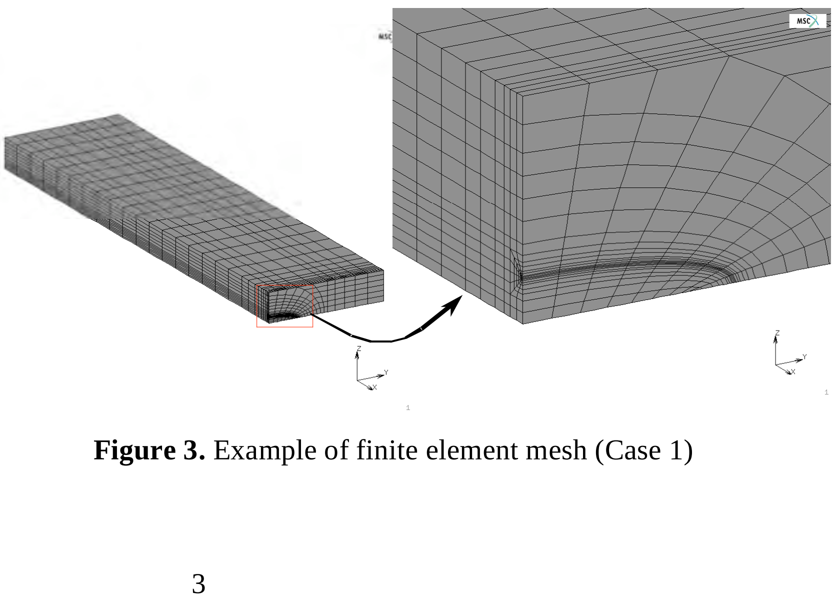

Figure 3. Example of finite element mesh (Case 1)

Table 1. Analysis condition

(a) Crack size

Case No.	Aspect ratio, a/c	Crack depth ratio, a/t	Crack length ratio, c/b
1	0.2	0.2	200
2	0.2	0.5	200
3	0.6	0.2	200
4	0.6	0.5	200

(b) Loading condition

Case No.	y-direction bending, S_{yb}, MPa	y-direction membrane, S_{ym}, MPa	x-direction membrane, S_x, MPa
A	200	0	0
B			100
C			-100
D		100	0
E			100
F			-100

Positive: Tensile, Negative: Compressive

Table 2. Material properties

Elastic-fully plastic	Young's modulus	E = 154,500 MPa
	Poisson's ratio	ν = 0.306
	Yield stress	σ_Y = 100 MPa
Elastic-plastic	Young's modulus	E = 154,500 MPa
	Poisson's ratio	ν = 0.306
	Yielsd stress	σ_Y = 109 MPa
	Stress-strain relation	$\varepsilon_p/\varepsilon_0 = \alpha\left(\sigma/\sigma_0\right)^n - \alpha \quad \left(\sigma \geq \sigma_Y\right)$ $\varepsilon_0 = 7.11\times10^{-4}$ $\alpha = 0.00274, \quad n = 5.05$

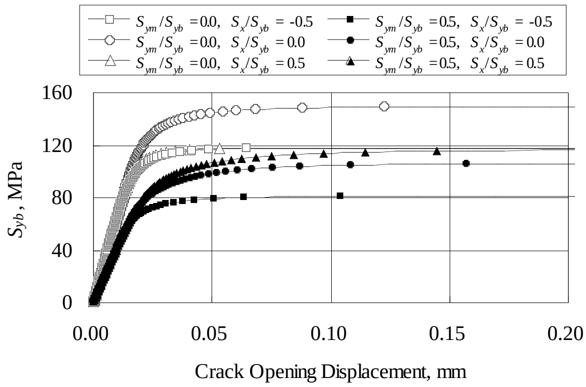

Figure 4. Example of S_{yb}-COD relation

(Case 1, a/c = 0.2, a/t = 0.5)

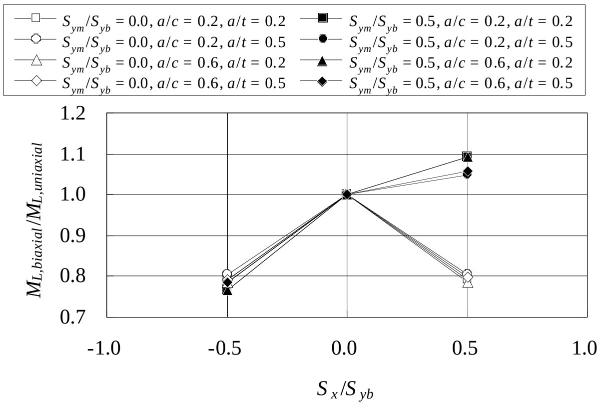

Figure 5. Normalized limit moment-S_x/S_{yb} relation

4.3 Results of elastic-plastic analysis

Example relations between J-integral at the deepest/surface points and S_{yb} are shown in Figs. 6 (a) and (b), respectively. J was evaluated as the path integral and the path-independency of J was individually confirmed. J is smoothly increasing with increasing S_{yb}, however, the increasing rate is affected by both S_{ym}/S_{yb} and S_x/S_{yb}, and the contribution of these parameters is not monotonic.

Figs. 7 (a) and (b) show the effect of S_x/S_{yb} on J at the final loading state (S_{yb} = 200 MPa). In a general way, J is not affected by S_x/S_{yb} for pure bending perpendicular to the crack, and J is decreasing with increasing S_x/S_{yb} for combined loading perpendicular to the crack. This implies that J could be evaluated by taking the effect of S_x/S_{yb} and S_{ym}/S_{yb} into account.

5 EXTENDED REFERENCE STRESS METHOD UNDER BIAXIAL LOADING

5.1 Limit moment solution under biaxial loading

Considering a plate with the yielding stress, σ_Y, being subjected to two components of principle stresses, σ_1 and σ_2, the Tresca yield criterion is expressed by

$$max\left(\left|\sigma_1\right|,\left|\sigma_2\right|,\left|\sigma_1-\sigma_2\right|\right)=\sigma_Y \tag{6}$$

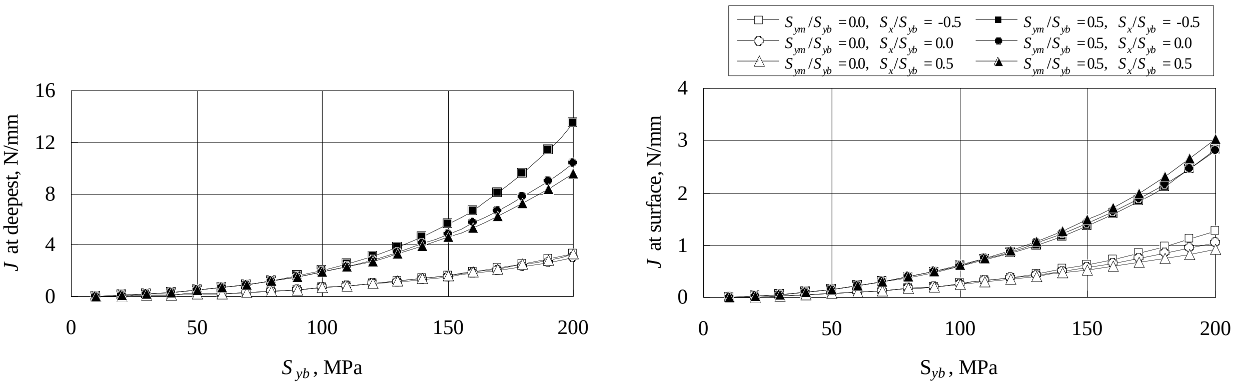

(a) at deepest point

(b) at surface point

Figure 6. Example of J-integral-S_{yb} relation (Case 1, a/c = 0.2, a/t = 0.5)

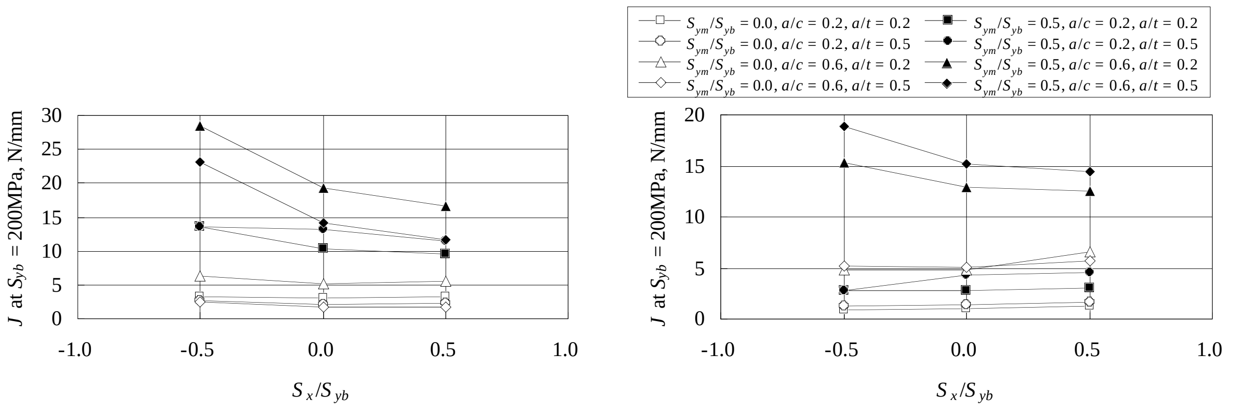

(a) at deepest point

(b) at surface point

Figure 7. J-integral at final loading state (S_{yb} = 200 MPa)-S_x/S_{yb} relation

As shown in Fig. 2, assuming that a surface cracked plate following elastic-perfectly plastic stress-strain response subjected to the remote bending stress, S_{yb}, and the remote membrane stress, S_{ym}, perpendicular to the crack, and the membrane stress parallel to the crack, S_x. The direction of S_x can be the same as σ_1, and the direction of S_{yb} and S_{ym} can be the same as σ_2, respectively. The limit load under biaxial loading can be determined so that it conforms to the Tresca yield criterion in eqn (6).

When S_x is tensile, the upper and lower admissible stresses are σ_Y and $-(\sigma_Y - S_x)$, as shown in Fig. 8 (a). Here the equilibrium equations on P and M_L are

$$P = 2\sigma_Y bu - 2\sigma_Y\left(1-s\right)b\left(t-u\right) = 2\sigma_Y b\left[\left(2-s\right)u - \left(1-s\right)t\right] \tag{7}$$

$$M_L = 2\sigma_Y b\int_0^u\left(\frac{t}{2}-x\right)d\xi + 2\sigma_Y\left(1-s\right)b\int_u^t\left(x-\frac{t}{2}\right)d\xi = \left(2-s\right)\sigma_Y bu\left(t-u\right) \tag{8}$$

where $s = S_x/\sigma_Y$, ξ is the coordinate along thickness direction, and u is the neutral location of the admissible stress distribution. Introducing the tension-bending ratio, Λ (= Pt/M), and the limit moment for uncracked plate, M_{L0}, defined in eqn. (4), above equations can be reduced to

$$\frac{M_L}{M_{L0}} = \frac{\left(1-s\right)\left(\sqrt{4+\Lambda^2}+2\right)}{\sqrt{\left(2-s-\frac{1}{2}s\Lambda\right)^2+\left(1-s\right)\Lambda^2}+\left(2-s-\frac{1}{2}s\Lambda\right)} \tag{9}$$

The stress parallel to the crack is not affected by the crack.

$$\sigma_1 = S_x \tag{10}$$

The stress perpendicular to the crack is affected by the existence of the crack, and the effect can be taken account through the reference stress, σ_{ref}, as a function of S_{yb} and S_{ym}.

$$\sigma_2 = \sigma_{ref}\left(S_{yb}, S_{ym}\right) \tag{11}$$

For simplicity, biaxial stress ratio parameter, $R_\sigma = S_x/S_{yb}$, and reference stress ratio parameter, $R_a = \sigma_{ref}/S_{yb}$, are introduced, principle stresses are then $\sigma_1 = R_\sigma S_{yb}$ and $\sigma_2 = R_a S_{yb}$. When a cracked plate satisfies the Tresca yield criterion, the upper admissible stress is

$$\sigma_Y = \sigma_{ref} \tag{12}$$

s is then equal to R_σ/R_a, and eqn (9) can be expressed as

$$\frac{M_L}{M_{L0}} = \frac{\left(R_a - R_\sigma\right)\left(\sqrt{4+\Lambda^2}+2\right)}{\sqrt{\left(2R_a - R_\sigma - \frac{1}{2}R_\sigma\Lambda\right)^2 + \left(R_a - R_\sigma\right)\Lambda^2} + \left(2R_a - R_\sigma - \frac{1}{2}R_\sigma\Lambda\right)} \tag{13}$$

When S_x is compressive, the upper and lower admissible stresses are $\sigma_Y + S_x$ and $-\sigma_Y$, as shown in Fig. 8 (b). Based on the similar procedure, limit moment solution under biaxial loading can be derived as

$$\frac{M_L}{M_{L0}} = \frac{\left(R_a + R_\sigma\right)\left(\sqrt{4+\Lambda^2}+2\right)}{\sqrt{\left(2R_a + R_\sigma - \frac{1}{2}R_\sigma\Lambda\right)^2 + \left(R_a + R_\sigma\right)\Lambda^2} + \left(2R_a + R_\sigma - \frac{1}{2}R_\sigma\Lambda\right)} \tag{14}$$

Thus eqns. (13) and (14) can be integrated as

$$\frac{M_L}{M_{L0}} = \frac{\left(R_a - |R_\sigma|\right)\left(\sqrt{4+\Lambda^2}+2\right)}{\sqrt{\left(2R_a - |R_\sigma| - \frac{1}{2}|R_\sigma||\Lambda|\right)^2 + \left(R_a - |R_\sigma|\right)\Lambda^2} + \left(2R_a - |R_\sigma| - \frac{1}{2}|R_\sigma||\Lambda|\right)} \tag{15}$$

In the above equation, the value of M_L/M_{L0} depends on the reference stress solution used to calculate R_a. For example, the solutions by Sattari-Far and Dillström (2004), and Lei (2004), which showed better agreement with finite element analysis results under uniaxial loading (see Figs. 1(a) to (b)), is used, R_a is given as

$$R_{a,Dillstrom} = \frac{2\left(1-\zeta\right)^{1.58} + \sqrt{4\left(1-\zeta\right)^{3.16} + \left(1-\zeta\right)^{3.14}\Lambda^2}}{6\left(1-\zeta\right)^2},\ \zeta = \begin{cases} \dfrac{a}{t}\dfrac{c}{c+t},\ for\ b \ge c+t \\ \dfrac{a}{t}\dfrac{c}{b},\ for\ b < c+t \end{cases} \tag{16}$$

$$R_{a,Lei} = \frac{2 + \frac{a}{t}\frac{c}{b}\Lambda + \sqrt{\left(2 + \frac{a}{t}\frac{c}{b}\Lambda\right)^2 + d_1\Lambda^2}}{6d_1},\ d_1 = \left(1 - \frac{a}{t}\frac{c}{b}\right)^2 + 2\left(\frac{a}{t}\right)^2\frac{c}{b}\left(1 - \frac{c}{b}\right) \tag{17}$$

The relations between M_L/M_{L0} and S_x/S_{yb} using eqns. (16) and (17) are shown in Figs. 9 (a) to (d) compared with those obtained from the elastic-perfectly plastic finite element analysis. Both of the reference solutions can express the qualitative contribution of S_x/S_{yb}. That is, M_L/M_{L0} takes the maximum value at $S_x/S_{yb} = 0$ and the contribution of S_x/S_{yb} is provided by its absolute value for pure bending perpendicular to the crack. In contrast, the contribution of S_x/S_{yb} is not symmetric and possible S_x/S_{yb} is not significantly affect M_L/M_{L0} for combined loading perpendicular to the crack. The proposed method generally smaller M_L/M_{L0} compared with the finite element analysis results when $S_x/S_{yb} \neq 0$. The predictive accuracy of the proposed method could be improved by use of the Mises yield criterion because it circumscribes the Tresca yield criterion.

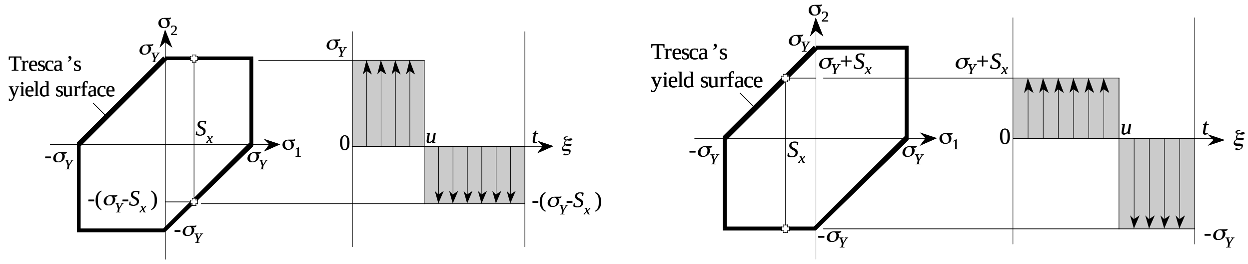

(a) for positive S_x (b) for negative S_x

Figure 8. Tresca yield states and associated stress distribution along thickness direction

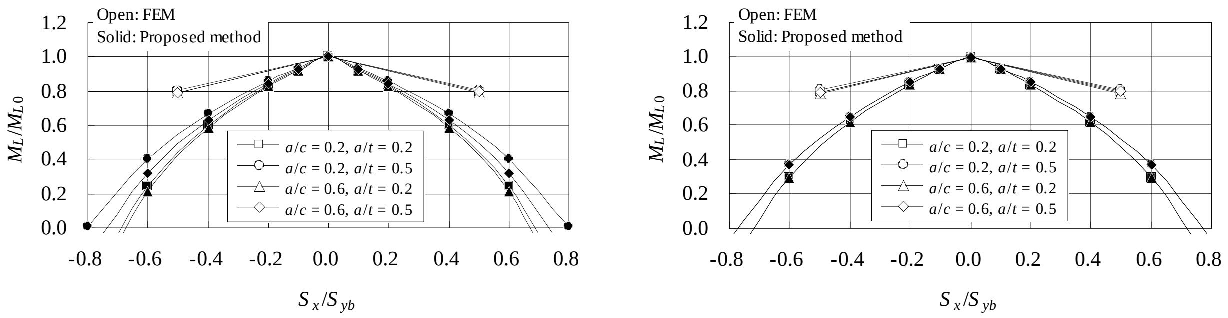

(a) Pure bending, Sattari-Far & Dillström (b) Pure bending, Lei

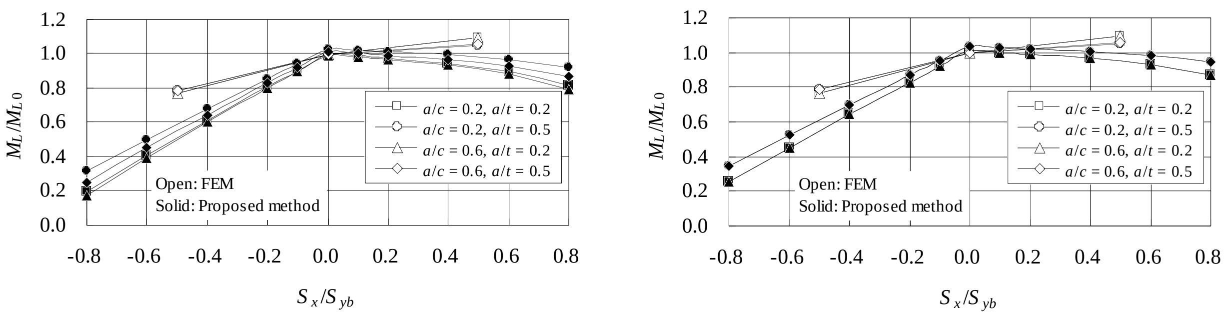

(c) Combined loading (Λ = 3), Sattari-Far & Dillström (d) Combined loading (Λ = 3), Lei

Figure 9. Comparison of M_L/M_{L0}- S_x/S_{yb} relations

5.2 Extended reference stress method under biaxial loading

Based on the reference stress method (Ainsworth, 1984), J-integral under elastic-plastic condition can be evaluated by the following equation,

$$J = \frac{E\varepsilon_{ref}}{\sigma_{ref}} J_e \tag{18}$$

where E is the Young's modulus, σ_{ref} and ε_{ref} are the reference stress and the reference strain, respectively. The elastic J-integral, J_e, is directly derived from the stress intensity factor, K_I, and is independent of the stress parallel to the crack.

$$J_e = \begin{cases} \left(1-\nu^2\right) K_I^{\,2} / E, & at\,deepest\ point \\ K_I^{\,2} / E, & at\,surface\ point \end{cases} \tag{19}$$

where ν is the Poisson's ratio. K_I for the plates with a semi-elliptical surface crack subjected to an arbitrary stress distribution can be calculated by the existing stress intensity factor solution (Chapuliot, 2000),

$$K_I = \left(\sigma_0 i_0 + \sigma_1 i_1 + \sigma_2 i_2 + \sigma_3 i_3\right)\sqrt{\pi a} \tag{20}$$

where i_l (l = 0 to 3) is the l-th order component of the nominal polynomial through-thickness stress representation and is tabulated as a function of a/c and a/t.

Postulating that the effect of biaxial loading can be properly taken account through the reference stress as the preceding discussion, it is expected that the reference stress method can be naturally extended under biaxial loading.

$$J = \frac{E\varepsilon_{ref,biaxial}}{\sigma_{ref,biaxial}} J_e \tag{21}$$

From eqns. (5) and (15), the reference stress under biaxial loading, $\sigma_{ref,biaxial}$, can be written as

$$\sigma_{ref,biaxial} = \frac{\sqrt{\left(2R_a - \left|R_\sigma\right| - \frac{1}{2}\left|R_\sigma\right|\left|\Lambda\right|\right)^2 + \left(R_a - \left|R_\sigma\right|\right)\Lambda^2} + \left(2R_a - \left|R_\sigma\right| - \frac{1}{2}\left|R_\sigma\right|\left|\Lambda\right|\right)}{6\left(R_a - \left|R_\sigma\right|\right)} S_{yb} \tag{22}$$

and $\varepsilon_{ref,biaxial}$ is the strain corresponding to $\sigma_{ref,biaxial}$ on the stress-strain relation.

5.3 Validation of proposed method

Figs. 10 (a) to (d) show the typical comparison of the relations between J-integral at the deepest/surface point and S_{yb}+S_{ym}, obtained from the proposed method together with the Lei's reference stress solution and finite element analysis. The proposed method gives a satisfactory prediction of J-integral both at the deepest and surface points. In the range of this evaluation (-0.5 ≤ S_x/S_{yb} ≤ 0.5, S_{yb} ≤ 2σ_Y), the significant effect of S_x/S_{yb} on J-integral is not observed both in finite element analysis and the prediction by the proposed method.

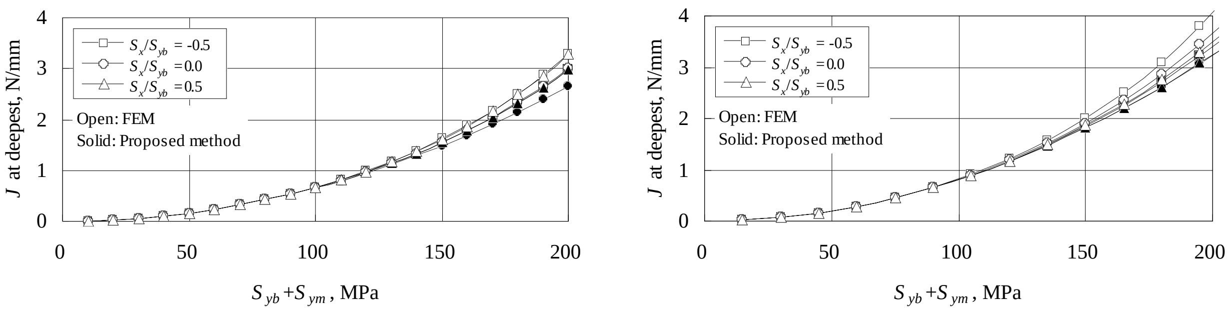

(a) Pure bending, at deepest point

(b) Combined loading (Λ = 3), at deepest point

Figure 10. Example comparison of J-integral-(S_{yb}+S_{ym}) relation (Case 1, a/c = 0.2, a/t = 0.5)

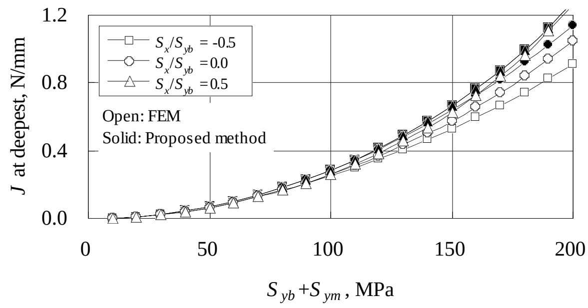

(c) Pure bending, at surface point

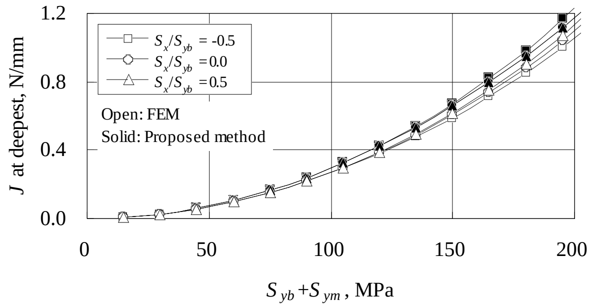

(d) Combined loading (Λ = 3), at surface point

Figure 10. Example comparison of J-integral-(S_{yb}+S_{ym}) relation (Case 1, a/c = 0.2, a/t = 0.5) (Cont'd)

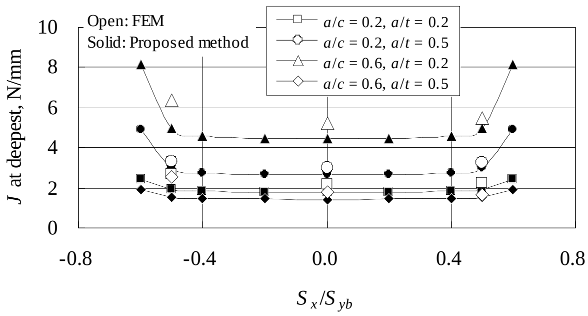

(a) Pure bending, at deepest point

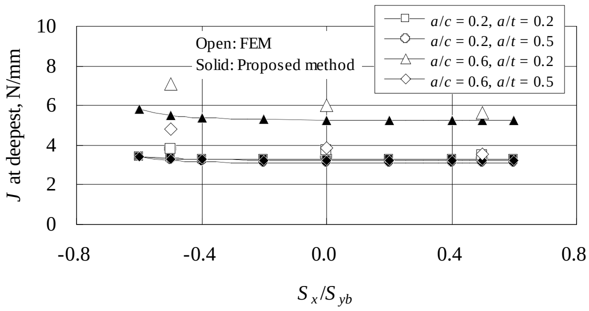

(b) Combined loading (Λ = 3), at deepest point

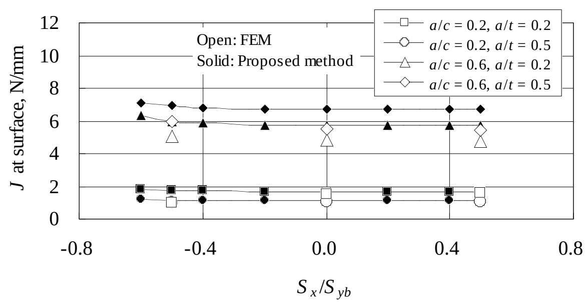

(c) Pure bending, at surface point

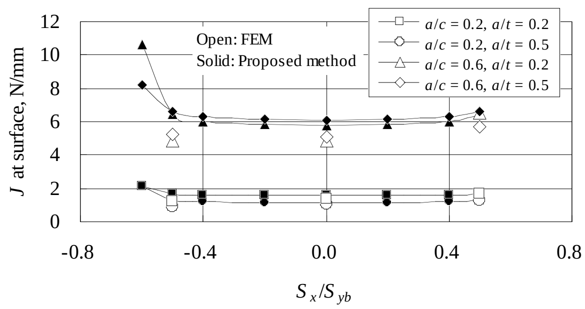

(d) Combined loading (Λ = 3), at surface point

Figure 11. Comparison of J-integral at S_{yb}+S_{ym} = 200 MPa

Figs. 11 (a) to (d) summarize the comparison of J-integral at the deepest/surface point at the total stress perpendicular to the crack (S_{yb}+S_{ym}) of 200 MPa. The J-integrals were evaluated by the proposed method together with the Lei's reference stress solution and finite element analysis. The effect of S_x/S_{yb} on J-integral can be well rationalized in spite of the differences in crack size. The proposed method generally gives higher J-integral compared with the finite element analysis, which leads to conservative prediction.

6 CONCLUSIONS

In this paper, existing reference stress solutions for plates with a semi-elliptical surface crack were reviewed. The applicability of the solutions was examined through the comparison with elastic-perfectly plastic three-dimensional finite element analysis results under uniaxial loading, and the solutions by Sattari-Far and Dillström, and by Lei could be the most appropriate reference stress solution. Next, a limit moment solution for cracked plates under biaxial loading was derived by modelling the Tresca yielding criterion under biaxial loading. An arbitrary combination of remote bending and tensile load perpendicular to the crack, and remote tensile/compressive load parallel to the crack can be taken into account. An extended reference stress method to evaluate J-integral under biaxial loading was then proposed based on the above limit moment solution. The applicability of the proposed method was validated through the comparison with elastic-plastic three-dimensional finite element analysis results. The proposed method could express the effect of the tensile/compressive load parallel to the crack on J-integral.

REFERENCES

Ainsworth, R. A. 1984. The Assessment of Defects in Structures of Strain Hardening Materials. Engineering Fracture Mechanics. Vol. 19. P. 633-642.

Chapuliot, S. 2000. Formulaire de K_I pour les tubes comportant un defaut de surface semi-elliptique longitudinal ou circonferentiel, interne ou externe. Rapport CEA-R-5900.

Goodall, I. W. and Webster, G. A. 2001. Theoretical Determination of Reference Stress for Partially Penetrating Flaws in Plates. International Journal of Pressure Vessels and Piping. Vol. 78. P. 687-695.

Lei, Y. 2004. J-Integral and Limit Load analysis of Semi-Elliptical Surface Cracks in Plates under Combined Tension and Bending. International Journal of Pressure Vessels and Piping. Vol. 81. P. 43-56.

Miura, N. and Takahashi, Y. 2007. Evaluation of J-Integral for Surface Cracked Plates under Biaxial Loading Using Extended Reference Stress Method. Proceedings of the 19th International Conference on Structural Mechanics in Reactor Technology. Vol. G.

Sattari-Far, I. 1994. Finite Element Analysis of Limit Loads for Surface Cracks in Plates. International Journal of Pressure Vessels and Piping. Vol. 57. P. 237-243.

Sattari-Far, I. and Dillstrom, P. 2004. Local Limit Load Solutions for Surface Cracks in Plates and Cylinders Using Finite Element Analysis. International Journal of Pressure Vessels and Piping. Vol. 81. P. 57-66.

Willoughby, A. A. and Davey, T. G. 1989. Plastic Collapse in Part-Wall Flaws in Plates. ASTM STP 1020. P. 390-409.